JCTC Journal of Chemical Theory and Computation

Transferability of Orthogonal and Nonorthogonal Tight-Binding Models for Aluminum Clusters and Nanoparticles

Ahren W. Jasper, Nathan E. Schultz, and Donald G. Truhlar*

Department of Chemistry and Supercomputing Institute, University of Minnesota, Minneapolis, Minnesota 55455-0431

Received August 10, 2006

Abstract: Several semiempirical tight-binding models are parametrized and tested for aluminum clusters and nanoparticles using a data set of 808 accurate Al_N ($N = 2-177$) energies and geometries. The effects of including overlap when solving the secular equation and of incorporating many-body (i.e., nonpairwise) terms in the repulsion and electronic matrix elements are studied. Pairwise orthogonal tight-binding (TB) models are found to be more accurate and their parametrizations more transferable (for particles of different sizes) than both pairwise and many-body nonorthogonal tight-binding models. Many-body terms do not significantly improve the accuracy or transferability of orthogonal TB, whereas some improvement in the nonorthogonal models is observed when many-body terms are included in the electronic Hamiltonian matrix elements.

I. Introduction

Atomistic simulations of large systems require methods for computing electronic energies and their gradients that are orders of magnitude more efficient than most ab initio and density functional theory (DFT) methods. Simple analytic potential energy functions (e.g., Lennard-Jones,[1] embedded atom,[2] etc.) are efficient, but they are not always accurate and may not be valid for uses other than those for which they are parametrized. For example, we showed previously[3,4] that analytic functions fit to either bulk data or diatomic data for pure aluminum perform poorly for particles of intermediate size, including clusters and nanoparticles. Although we were able to obtain[4] analytic potential energy functions that are accurate for small clusters, nanoparticles, and bulk aluminum using reasonably simple functional forms and an efficient fitting strategy that includes both small clusters and the bulk, the problem of extending these fits to heteronuclear systems remains unsolved and would likely require modified functional forms, such as charge-transfer terms,[5] variable atom types,[6] and so forth.

Semiempirical molecular orbital or crystal orbital methods include extended Hückel theory,[7] tight binding[8] (which is simply a more flexible form of extended Hückel theory or another name for extended Hückel theory), and neglect of differential overlap theories (like AM1[9,10] and others which have recently been reviewed[11]). They offer a theoretically attractive approach to modeling reactive systems because they are computationally affordable for many systems, while they include an orbital-based Hamiltonian, a diagonalization step, and the Pauli principle, three features that give rise to directional bonding and valence saturation. Some such methods, for example, Hoffmann's extended Hückel method,[7] include orbital overlap both in parametrizing the Hamiltonian and in the secular equation, while other methods, both in physics and in chemistry, include orbital overlap (or a function with comparable dependence on interatomic distance) in the Hamiltonian, but not in the secular equation. (The original Hückel method, in which the Hamiltonian matrix elements were constants, is no longer widely used.) Methods that neglect overlap in the secular equation are usually labeled "orthogonal", whereas those that retain it in the secular equation are labeled "nonorthogonal", and we follow this usage here. Molecular orbital methods provide a natural energetic description of bond breaking and forming and many-body effects.

Another classification that may be made is based on whether a method is designed to include self-consistent (i.e., iterative) steps, which may be necessary for accurately

* Corresponding author. Fax: (612) 624-7007. E-mail: truhlar@umn.edu.

10.1021/ct600261s CCC: $37.00
Published on Web 12/08/2006

modeling charge transfer and polar bonds. Although the motivation is to eventually use orbital methods to model Al heteronuclear chemistry, the focus of the present work is limited to pure aluminum clusters and nanoparticles where charge transfer and bond polarity may be expected to be less important than other contributions to the total energy, and we therefore restrict our attention in the present article to noniterative methods without an explicit treatment of charge interactions.

Popular orbital-based semiempirical methods were tested recently[12] for small aluminum clusters, where it was found that none of the semiempirical methods tested was accurate enough for quantitative work. The most accurate semiempirical method tested in ref 12 (AM1,[9,10] which involves iterating to self-consistency) had an average error of ~0.3 eV/atom. Subsequently, several parametrizations based on the Wolfsberg−Helmholtz[13] (WH) tight-binding (TB) model were obtained[14] using a database of aluminum cluster Al_N ($N = 2-13$) energies with an average error as small as 0.03 eV/atom. Here, we build on that work and explicitly consider the transferability of TB parametrizations using an expanded data set, containing systems as large as 177 atoms. We also consider both orthogonal and nonorthogonal TB models, and we discuss the relationship between orthogonality and many-body effects.

The question of orthogonal versus nonorthogonal formulations also arises in semiempirical methods that include a self-consistent-field step. For example, AM1[9,10] and PDDG/PM3[15] both set the overlap matrix equal to unity in the secular equation, whereas SCC-DFTB[16,17] and NO-MNDO[18] include the overlap matrix in the secular equation, thereby increasing the cost. Nonorthogonal formulations also complicate the gradient calculation,[19] and they make it more difficult to achieve linear scaling of computational times for large systems, although linear-scaling nonorthogonal formulations have been presented for both non-self-consistent[20,21] and charge-self-consistent[22] tight-binding methods. A recent[23] study found that the mean unsigned error for the heat of reaction of 34 diverse isomerization reactions is 7.1, 5.0, and 2.8 kcal/mol (0.31, 0.22, and 0.12 eV) for AM1, SCC-DFTB, and PDDG/PM3, respectively. Similar results were found for 622 heats of formation, with the nonorthogonal SCC-DFTB intermediate in accuracy between AM1 and PDDG/PM3[23] and with NO-MNDO better than MNDO for HCO compounds but not for HCN compounds.[18] Thus, orthogonal formulations may be either less or more accurate than nonorthogonal ones, depending on the parametrization. The present study is designed to test the role of nonorthogonality in tight-binding theory by parametrizing nonorthogonal and orthogonal formulations in the same way using the same training data.

Section II briefly introduces the TB models that are considered in this paper. In section III, the database of accurate energies is described, and the TB models are parametrized and tested in section IV. Section V discusses the results, and section VI is a summary.

II. Theory

A many-electron molecular wave function may be approximated as a product of one-electron wave functions ψ_j that satisfy

$$\hat{H}\psi_j = \epsilon_j\psi_j \tag{1}$$

where

$$\hat{H} = \hat{T} + \hat{V}_{\mathrm{NE}} + \hat{V}_2 \tag{2}$$

$\hat{T}$ is the kinetic energy operator; $\hat{V}_{\mathrm{NE}}$ is the Coulomb operator for the attraction of the electron to all of the nuclei, and $\hat{V}_2$ is the sum of the two-electron operators for the Coulomb repulsion, exchange, and correlation. We treat the valence electrons explicitly and combine the core electrons with the nuclei as the total core.

To solve eq 1, the one-electron molecular orbitals ψ_j are expanded in an atomic orbital basis set φ_μ^k, where i labels the individual atomic orbitals centered on atom k

$$\psi_j = \sum_i c_{ij}\varphi_i \tag{3}$$

where $i \equiv (\mu,k)$. The optimal expansion coefficients are obtained by solving the secular equation

$$\mathbf{Hc} = \epsilon\mathbf{Sc} \tag{4}$$

where ϵ is a diagonal matrix with diagonal elements ϵ_j

$$H_{\mu\mu'}^{kk'} = \langle\varphi_\mu^k|\hat{H}|\varphi_{\mu'}^{k'}\rangle \tag{5}$$

and

$$S_{\mu\mu'}^{kk'} = \langle\varphi_\mu^k|\varphi_{\mu'}^{k'}\rangle \tag{6}$$

The sum of the orbital energies (the eigenvalues of eq 4) weighted by the appropriate orbital occupancies n_j (with $n_j = 0$, 1, or 2, where j labels the eigenvalues and eigenvectors) is called the valence energy or the band energy, given by

$$E_{\mathrm{Val}} = \sum_j n_j\epsilon_j \tag{7}$$

Energy levels are typically filled to minimize eq 7, which is called the aufbau principle. However, in some cases, it is useful to minimize a more general electronic energy given by

$$E_{\mathrm{Elec}} = E_{\mathrm{Val}} + \delta_{n_j2}U_{\mathrm{Pen}} \tag{8}$$

where U_{Pen} is a penalty energy[24] for pairing electrons. We consider several values of the penalty energy (including zero). The use of a penalty energy is operationally equivalent to having different Hamiltonians for spin-up and spin-down electrons, where the Hamiltonians differ only in that U_{Pen} is added to the diagonal for spin-down electrons.

The total energy E is

$$E = E_{\mathrm{Elec}} + E_{\mathrm{Core}} - E_{\mathrm{DC}} \tag{9}$$

where E_{Core} is the core−core repulsion and E_{DC} corrects for the double counting of the two-electron interactions $\hat{V}$. The double-counting term and the core−core repulsion are often

grouped together and represented by an effective pairwise repulsive term

$$E = E_{\mathrm{Elec}} + V_{\mathrm{Rep}} \tag{10}$$

The pairwise form for V_{Rep} has been justified by Foulkes and Haydock.[25] We use a three-parameter repulsion with the form

$$V_{\mathrm{Rep}} = \sum_{k<k'} A \exp(-BR_{kk'})/R_{kk'}^{C} \tag{11}$$

where $R_{kk'}$ is the distance between atoms k and k'; A, B, and C are parameters; and the summation runs over all unique pairs of atoms.

In semiempirical tight-binding models, several additional approximations are made to make the above procedure computationally efficient. First, a minimal basis set is employed (specifically, for Al, one 3s and three 3p orbitals per atom). Next, the matrix elements $H_{\mu\mu'}^{kk'}$ are taken as empirical parameters or simple functions of empirical parameters. In this article, we consider the WH[13] model where

$$H_{\mu\mu'}^{kk} = -\delta_{\mu\mu'} U_{\mu}^{k} \tag{12}$$

U_{μ}^{k} is the valence state ionization potential for an electron

$$H_{\mu\mu'}^{kk'} = K\frac{H_{\mu\mu}^{kk} + H_{\mu'\mu'}^{k'k'}}{2} S_{\mu\mu'}^{kk'} \quad (k \neq k') \tag{13}$$

in atomic orbital i on atom k, and K is an empirical parameter, which Hoffmann optimized[7] to 1.75 but which we take to be a fitting parameter. We consider two other models for the off-diagonal elements: a parameter-free model derived by Cusachs and Cusachs[26] (CC)

$$H_{\mu\mu'}^{kk'} = (2 - |S_{\mu\mu'}^{kk'}|)\frac{H_{\mu\mu}^{kk} + H_{\mu\mu}^{k'k'}}{2} S_{\mu\mu'}^{k'k'} \tag{14}$$

and a form proposed by Lathiotakis et al.[27] for metals, which we denote LAMC.

In the present study, the valence state ionization potentials U_i^k used in eq 12 are fixed at the atomic experimental[28] values (10.62 and 5.986 eV for the 3s and 3p orbitals, respectively). Then, along with the three parameters in the repulsion, the WH model has one adjustable parameter K; the CC model has no adjustable parameters, and the LAMC model has five adjustable parameters for Al. Following Slater and Koster,[8] the matrix elements were evaluated in a symmetry-adapted local coordinate system when computing eq 14.

In all of the above formulations, $H_{\mu\mu'}^{kk'}$ depends only on atoms α and β, whereas in a more accurate calculation, the one-electron contributions also involve three-center terms, and the two-electron contributions involve three- and four-center terms. Slater and Koster[8] suggested the two-center simplification, and it is widely used. The models discussed above are usually called nonorthogonal tight-binding (NTB) to emphasize the retention of the overlap matrix **S**.

One may choose to go beyond pairwise tight binding by writing $H_{\mu\mu'}^{kk'}$ or V_{Rep} as a function of the geometry of the entire system (or the local geometry), and we call such formulations many-body tight-binding (MBTB) models.[14] (Some workers[29−33] call them environmental-dependent tight binding.) Ho and co-workers[30−32] suggested a many-body term to model screening. The screening many-body term was tested previously for WH tight binding for aluminum clusters,[14] and it was shown to be more accurate than two other many body-terms that were also tested. In the present article, we consider three implementations of the screening (S) many-body function, applied (as discussed elsewhere[14]) to screening the repulsion (SR), screening the ionization potentials (SIP), or screening the off-diagonal elements (SOD). The screening many-body function has three fitting parameters, and the SIP implementation has two additional parameters, as discussed elsewhere.[14] The many-body terms also contain a two-parameter cutoff function, as discussed in ref 3. One may call a model that retains overlap and adds many-body terms "nonorthogonal many-body tight-binding" (NMBTB).

Finally, one may also choose to neglect the overlap when solving eq 4, and we denote these models as TB and many-body tight binding; one could also say orthogonal tight-binding and orthogonal many-body tight-binding, but the usual notation in the literature is to assume orthogonality when "nonorthogonal" is not specified. There has been work[34] showing that the effect of including overlap (as in NTB) is similar to including a many-body term in the off-diagonal matrix elements of a TB model. This leads to the interpretation that NTB is more accurate than TB because it effectively goes beyond the pairwise approximation. However, both TB and NTB involve a diagonalization step, and therefore, both schemes include many-body effects. Furthermore, if one chooses to view eq 10 as a fitting scheme, then V_{Rep} not only includes the double-counting correction and the core−core repulsion, but it also empirically corrects for all of the other approximations made when applying TB to real systems. As a result, although it is true that the overlap matrix is very different from the unit matrix at chemical atom−atom separations, in light of the many other significant approximations in TB and NTB theory, it is not clear how important it is to include overlap in the secular equation. The question of whether one achieves a better *balance* of approximations when one retains or neglects overlap is one motivation for the current work.

III. Calculations

The tight-binding models are tested using the previously presented pure aluminum nanoparticle data set.[4] This data set consists of 808 energies and geometries for Al_N, with $N = 2-177$, including 127 data points for particles with diameters greater than 1 nm. Symmetric structures such as icosahedral, face-centered cubic (FCC), hexagonal close-packed, body-centered cubic, and simple cubic are included for several atomic volumes. Nonsymmetric structures are represented as well, including disordered structures and structures with over- and undercoordinated interior atoms, that is, atoms with coordination numbers greater than and less than the bulk value of 12. The data set is divided into 11 groups containing particles with sizes $N = 2$, 3, 4, 7,

Table 1. Mean Unsigned Errors (eV) for Several Tight-Binding (TB) Parameterizations[a]

method	fitting data	U_{Pen}, eV	K	ϵ_{Dim}	ϵ_{Clus}	ϵ_{Nan}	ϵ
WH	2	0	0.38	0.03	0.07	0.06	0.06
	2−13	0	0.41	0.03	0.06	0.06	0.06
	2−177	0	0.41	0.03	0.06	0.05	0.05
	2	0.02	0.39	0.02	0.07	0.06	0.06
	2−13	0.05	0.41	0.03	0.05	0.06	0.06
	2−177	0.04	0.41	0.03	0.06	0.05	0.05
	2	3	0.51	0.04	0.42	0.76	0.57
	2−13	3	0.42	0.10	0.10	0.09	0.09
	2−177	3	0.44	0.11	0.11	0.05	0.08
WH+SIP	2−13	0	0.40	0.03	0.06	0.06	0.06
WH+SR	2−13	0	0.43	0.04	0.05	0.05	0.05
WH+SOD	2−13	0	0.41	0.03	0.05	0.06	0.06
LAMC	2	0		0.03	1.89	3.81	2.77
	2−13	0		0.09	0.07	0.12	0.10

[a] All errors are averages over all 11 groups of data, even though the fits to the $N = 2$ data and the $N = 2-13$ data use only one or five, respectively, of the groups for fitting.

Table 2. Mean Unsigned Errors (eV) for Several Nonorthogonal Tight-Binding (NTB) Parametrizations

method	fitting data	U_{Pen}, eV	K	ϵ_{Dim}	ϵ_{Clus}	ϵ_{Nan}	ϵ
WH	2	0	1.85	0.08	0.63	1.20	0.89
	2−13	0	1.91	0.27	0.31	0.49	0.40
	2−177	0	1.99	0.38	0.41	0.24	0.31
	2	4.54	1.52	0.01	1.14	2.42	1.73
	2−13	0.24	1.91	0.24	0.30	0.44	0.37
	2−177	0.20	1.99	0.35	0.41	0.21	0.30
WH+SIP	2−13	0	1.94	0.15	0.20	0.40	0.30
WH+SR	2−13	0	1.89	0.24	0.31	0.44	0.37
WH+SOD	2−13	0	1.86	0.14	0.25	0.23	0.23
WHXR	2	0	1.61	0.28	0.70	1.21	0.94
	2−13	0	1.77	0.34	0.54	0.70	0.61
	2−177	0	1.90	0.49	0.70	0.35	0.49
CC	2	0		0.13	0.52	1.10	0.80
	2−13	0		0.16	0.49	1.10	0.79
	2−177	0		0.18	0.49	1.08	0.79
CCXR	none	0		0.19	0.50	1.08	0.79

Table 3. Mean Unsigned Errors (eV) for Several Previously Presented Parameterizations for Pure Aluminum

method (ref)[a]	fitting data	U_{Pen}, eV	K	ϵ_{Dim}	ϵ_{Clus}	ϵ_{Nan}	ϵ
ER (3)	2			0.01	0.82	2.75	1.80
Gol (36)	bulk			0.12	0.12	0.13	0.12
NP-A (4)	2−177			0.01	0.08	0.03	0.05
NP-B (4)	2−177			0.09	0.08	0.05	0.06
WH (14)	2−13[b]	0.07	0.39	0.03	0.06	0.06	0.06
OWH (14)	2−13[b]	0.07	*c*	0.06	0.08	0.07	0.07
EWH (14)	2−13[b]	0.07	*c*	0.05	0.06	0.09	0.08
MBTBS (14)	2−13[b]	0.07	*c*	0.02	0.05	0.08	0.06
MBTBCN (14)	2−13[b]	0.07	*c*	0.03	0.07	0.09	0.08
MBTBBA (14)	2−13[b]	0.07	*c*	0.03	0.05	0.06	0.06

[a] Reference number in parentheses. [b] A subset of the current data set for Al_N, $N = 2-13$, was used for these fits. [c] These models have multiple values of K, depending on the local orbital symmetry.

9−13, 14−19, 20−43, 50−55, 56−79, 80−87, and 89−177, and the number of data points in each group is 44, 402, 79, 42, 72, 42, 46, 23, 27, 15, and 16, respectively.

Mean unsigned errors per atom for each data group are computed as discussed elsewhere.[4] As we are interested in the transferability of the TB parametrizations for different particle sizes, we further average the errors and report the mean unsigned error ϵ_{Dim} for the dimer data, the average ϵ_{Clus} of the mean unsigned errors for the four groups containing aluminum clusters with sizes between 3 and 13 atoms, and the average ϵ_{Nan} of the mean unsigned errors for the six groups of nanoclusters and nanoparticles containing between 14 and 177 atoms. The overall mean unsigned error ϵ is obtained by averaging all 11 data groups, which is equivalent to

$$\epsilon = (\epsilon_{Dim} + 4\epsilon_{Clus} + 6\epsilon_{Nan})/11 \quad (15)$$

The available adjustable parameters were optimized by minimizing ϵ_{Dim}, $(\epsilon_{Dim} + 4\epsilon_{Clus})/5$, or ϵ using a genetic algorithm[35] for two values of the penalty energy U_{Pen}, 0 or 3 eV. Fits were also obtained by treating the penalty energy as an optimized fitting parameter.

IV. Results

Once the optimal parameters were obtained, the resulting fits were then tested against the full data set, and the results are summarized in Tables 1 and 2. For comparison, Table 3 contains errors for several fits that have previously appeared in the literature, including four analytic potential energy functions: ER,[3] a pairwise form fit to the aluminum dimer; Gol,[36] an embedded-atom form fit to bulk data; and NP-A and NP-B,[4] the two most accurate analytic potential energy functions from ref 2 fit to the same data set that is used here. Also shown in Table 3 are six tight-binding fits obtained previously[14] using a subset of the current data set with Al_N, $N = 2-13$, as well as a data set of ionization potentials and bulk properties. The OWH and EWH models are TB models that may be considered as extensions of the WH model, and the MBTBS, MBTBCN, and MBTBBA are examples of MBTB, in particular WH models with screening (S) and two other types (CN and BA) of many-body terms.[14]

V. Discussion

First, we consider the TB and MBTB results in Table 1. For zero penalty energy and when the penalty energy is optimized (resulting in values of 0.02 to 0.05 eV), the parametrizations obtained by fitting *only* to dimer data give very good overall errors of 0.06 eV/atom. When parameters are obtained by fitting to the full data set of 808 geometries, the overall errors do not improve significantly. Furthermore, these errors (∼0.05 eV/atom) are close to the error for the most accurate of the orthogonal fits and analytic potential energy functions presented previously[4,14] (see Table 3). This is perhaps a surprising result considering the long list of approximations involved in the simple, four-parameter, orthogonal WH TB model and that the training set involves no information about many-body effects.

Fits obtained with a penalty energy of 3 eV, which is the value used by Wang and Mak,[24] have larger errors than those

for smaller penalty energies. Furthermore, the transferability of the resulting fits is not as good as is observed for smaller penalty energies; that is, the errors are significantly larger for data not included in the fits when a subset of data is used as fitting data.

Including many-body terms (as in the SIP, SR, and SOD models) does not significantly improve the overall error, and this is likely due to the already excellent performance with accurate pairwise interactions.

The optimal value of the Wolfsberg-Hemlholtz parameter K is around 0.4 for the more accurate TB fits, which is very different from the value of 1.75 used by Hoffmann.[7] The value of 1.75 was obtained in the context of NTB, where Hoffmann gave an argument[7] that K should be greater than unity. In the context of orthogonal TB there is no such restriction, and the present values of $\sim$0.4 are therefore reasonable.

We also tested the LAMC functional form for the TB model. As shown in Table 1, the dimer LAMC fit does not show the excellent transferability of the WH model, although by fitting to data up to Al_{13}, good transferability is obtained to the regime of larger clusters and nanoparticles.

Next, we consider the NTB models summarized in Table 2. The overall errors for the pairwise NTB fits are in the range 0.3−1.7 eV/atom. The parametrizations obtained by fitting to the dimer data perform poorly for larger clusters. For example, the WH NTB model with zero penalty energy fits the dimer data with an error of 0.08 eV/atom, which is only slightly worse than the best TB model in Table 1. But when this parametrization is used to model clusters and nanoparticles, the mean unsigned error increases by factors of 8 and 16, respectively, resulting in qualitatively incorrect fits.

Many-body terms were incorporated in the nonorthogonal formalism, and their parameters were fit to the dimer and cluster data; after which, the resulting fits were tested against the full data set. Table 2 indicates that the presence of the many-body terms in the repulsion (WH+SR) does not significantly improve the nonorthogonal model. Adding terms in the electronic part of the calculation, however, is more useful, and the errors for the Al_N data with $N = 2-13$ decrease by 24% and 37% for the SOD and SIP models, respectively, compared to the pairwise NTB fits. When the NMBTB models are tested for transferability against the larger cluster and nanoparticle data, the SOD model is the most accurate. However, even the best NMBTB method (WH+SOD) has an error that is 4−5 times greater than that of the simplest TB method.

Tight binding is sometimes implemented without explicit repulsion, and theoretical arguments may be given in support of this choice.[7,37] (Other workers find it more natural to retain explicit core repulsion.[38]) One may wonder if including an empirical repulsion during the fitting procedure is perhaps responsible for the lack of transferability of the NTB parametrizations. (Note that removing the repulsion cannot make the fitted errors decrease, as the resulting model is less flexible. We are simply testing the effect that the repulsion has on the transferability of the NTB parametrizations.) We fit three NTB WH models without repulsion (denoted "XR"), and the results are shown in Table 2. We find that the trends are similar for NTB with and without repulsion, and that, in fact, NTB with repulsion has slightly better transferability.

The CC TB model has no parameters in the electronic part of the calculation, and three CC NTB fits were obtained. The CC model without repulsion (CCXR) has no adjustable parameters, and its errors are also presented in Table 2. For the CC model, the repulsion does not significantly improve the fitting error or the transferability. The overall errors for the CC methods are larger than those for the best WH NTB fits.

Comparing the best TB to NTB parametrizations shows that the TB models are both more accurate and more transferable than the NTB ones. Several theoretical analyses of the effect of including the overlap in TB have appeared in the literature,[7,25,26,30−33,39−43] many of which focus on the bulk band structure. We do not attempt another such analysis here, but we do note that, whenever the effect of including overlap has been discussed, there is an implicit assumption or explicit working hypothesis, sometimes based on experience, that including overlap should make the model more realistic. This belief also underlies discussions of other forms of semiempirical molecular orbital theory; for example, the statement that overlap introduces many-body effects was used to justify its inclusion in a self-consistent-charge density-functional tight-binding scheme.[16,17] However, we know of no previous systematic test as extensive as the present one.

Although it would be hard to establish firm guidelines for the inclusion of overlap, we can illustrate the qualitative difference in the TB and NTB WH dimer, and this is done in Figures 1 and 2. Figure 1b shows that the electronic eigenvalues have a qualitatively different shape for NTB and TB, even for the dimer curve. For the TB model, at $R = 2.8$ Å, the 3s and 3p energy bands are split by 1.9 and 1.6 eV, respectively. For the NTB model, the bands split by 3.5 and 8.6 eV, respectively, and several of the energy levels tend toward positive numbers at small atom−atom separations. One can explain this qualitative difference as resulting from terms such as $(1 - S^{kk'}_{\mu\mu'})$ in the denominator of the NTB energy expressions, whereas these terms are absent in the TB model. For the aluminum dimer, the energy levels that tend to large positive numbers are not occupied (for zero penalty energy), the filled energy levels have similar shapes for the TB and NTB models, and both models are able to fit the aluminum dimer data with good accuracy.

Figure 2 shows the energetics for an FCC Al_{13} cluster as a function of the distance of all 12 surface atoms from the central atom for the same two fits as were shown in Figure 1. The TB total energy is fairly accurate, with the minimum occurring very close to the accurate minimum. The NTB total energy is qualitatively incorrect. Figure 2b shows the qualitative behavior of the eigenvalues, which is similar to the behavior of the eigenvalues for the dimer. In the case of Al_{13}, however, some of the repulsive electronic energy levels for NTB are occupied, leading to an NTB total energy that is too high for Al_{13}. It is interesting to note that the electronic energy E_{Elec} for the NTB method is in qualitative agreement with the accurate total energy E.

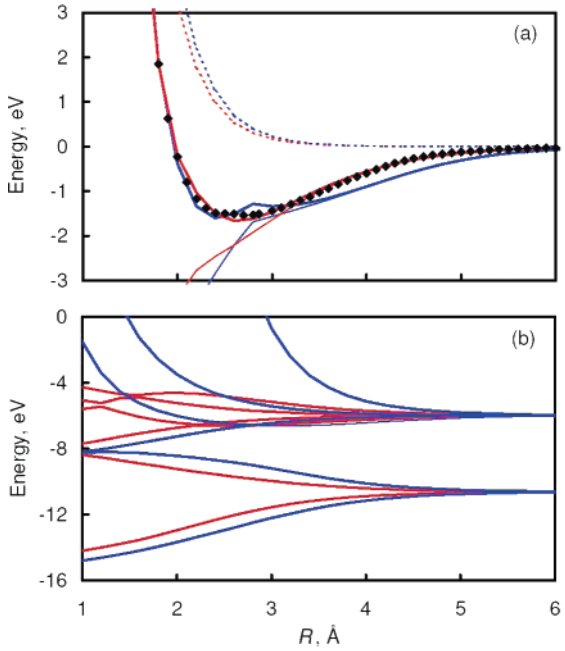

Figure 1. (a) Repulsive (thin dashed) and electronic (thin solid) components of the total energy (thick solid) for the aluminum dimer as a function of the nearest-neighbor distance R for TB (red) and NTB (blue) models. The accurate (PBEh/MG3 from ref 4) total energies are shown as black diamonds. (b) Electronic energy levels ϵ_j for TB (red) and NTB (blue) models of the aluminum dimer. Some of the levels are degenerate. For zero penalty energy, half the levels are filled.

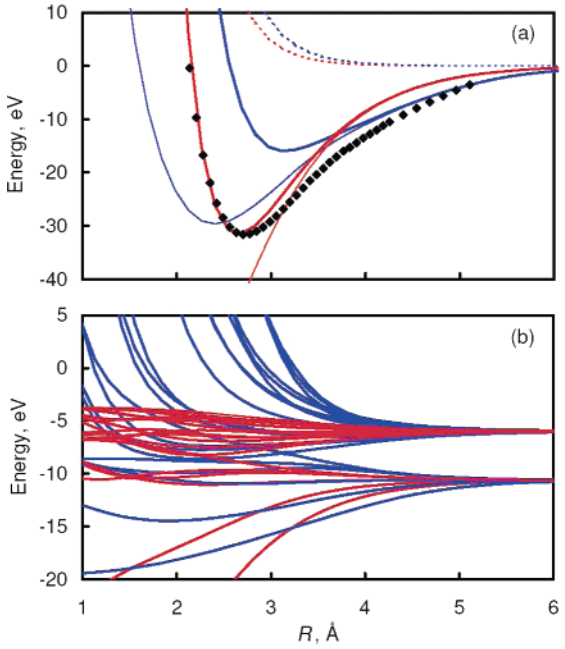

Figure 2. (a) Repulsive (thin dashed) and electronic (thin solid) components of the total energy (thick solid) for a face-centered cubic cluster of Al_{13} as a function of the nearest-neighbor distance R for TB (red) and NTB (blue). The accurate (PBEh/MG3 from ref 4) total energies are shown as black diamonds. (b) Electronic energy levels for TB (red) and NTB (blue) for the aluminum dimer. Some of the levels are degenerate. For zero penalty energy, half the levels are filled.

To gain further insight, we compare tight binding with DFT. The level of theory is unrestricted PBEh/MEC,[44,45] and the electronic (band) energy of DFT is defined as

$$E_{\mathrm{Elec}} = \sum_{\gamma=\alpha,\beta} \sum_{j} n_j^{\gamma} \epsilon_j^{\gamma} - E_0 \qquad (16)$$

where γ denotes spin, ϵ_j^{γ} is the DFT orbital eigenvalue, n_j^{γ} is the orbital occupancy (0 or 1), and E_0 sets the zero of energy. (Note that PBEh was formerly called PBE0.) We define the correction term to the electronic energy as

$$V_{\mathrm{Rest}} = E - E_{\mathrm{Elec}} - E_0 \qquad (17)$$

where E is the DFT total energy. The correction term includes core−core repulsion and the double counting correction for the electronic Coulomb interactions. We set E_0 such that V_{Rest} is zero for N infinitely separated atoms, that is, $E_0 = N(E^1 - E_{\mathrm{Elec}}{}^1)$, where E^1 and $E_{\mathrm{Elec}}{}^1$ are E and E_{Elec} for an isolated Al atom, respectively, and N is the number of atoms in the system.

Figure 3 shows V_{Rest} for PBEh/MEC and V_{Rep} for TB and NTB, scaled (as explained in the caption) by the reciprocal of the number N of atoms. Near equilibrium, V_{Rest} is approximately 3.7 and 2.5 times larger than V_{Rep} for TB and NTB, respectively. Some of the structure in the DFT Al_{13} curve is due to the lowest-energy solution changing its multiplicity as a function of nearest-neighbor separation.

Figure 4 shows the $4N$ lowest orbital energies (averaged over α and β spin for the case with an odd number of electrons and for distances where the dimer is a triplet) for

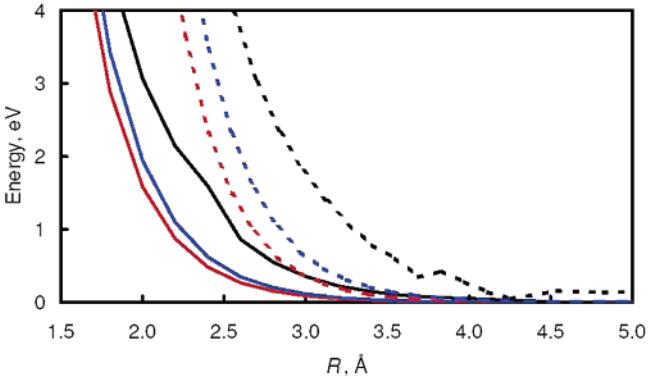

Figure 3. V_{Rep}/N for TB (red) and NTB (blue) and V_{Rest}/N for DFT (black) for aluminum dimer (solid) and FCC Al_{13} (dashed) as a function of nearest-neighbor distance R. The DFT method used for this figure is PBEh/MEC.

DFT (in particular, PBEh/MEC) calculations on Al_2 and for FCC Al_{13}. (Notes: (i) because MEC denotes the usage of an effective core potential, there are no core orbitals in a PBEh/MEC calculation, and this is equivalent to the $4N$ lowest-energy valence orbitals in an all-electron calculation; (ii) in counting to $4N$, degenerate orbitals are counted a number of times equal to their degeneracy, but we still have eight curves at some internuclear distances R for Al_2 because when the triplet is lower than the singlet for Al_2 we use the triplet solution, which breaks the degeneracy of the π orbitals in the unrestricted self-consistent-field formalism used here.) Quantitative comparisons between DFT and tight binding are not possible because of the different approximations

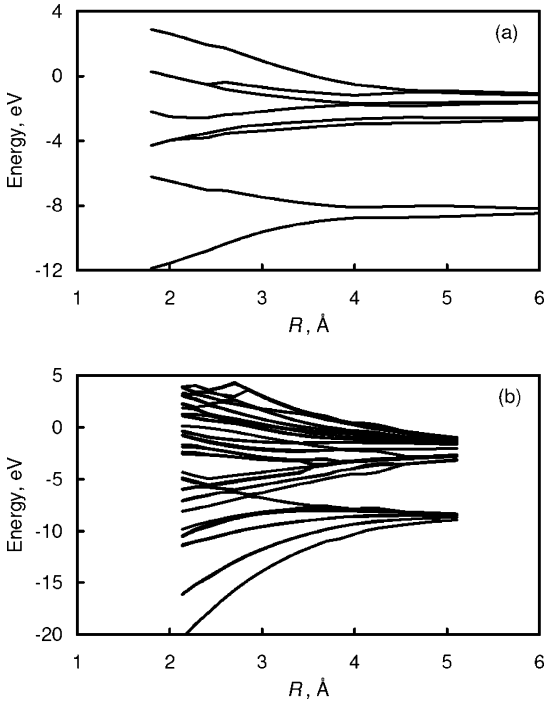

Figure 4. Electronic energy levels for DFT for (a) the aluminum dimer and (b) a face-centered cubic cluster of Al_{13} as a function of the nearest-neighbor distance R. The DFT method used for this figure is PBEh/MEC.

involved in the two theories. For example, for infinitely separated atoms, the TB and NTB energy levels give (by construction) the experimental ionization potentials, and the pairwise repulsion (again, by construction) goes to zero. In the DFT calculation, however, the energy levels for separated atoms include double counting of the Coulomb terms, and therefore, the correction term to the sum of the occupied orbital energies is not zero. We have taken account of this by our choice of the zero of energy in Figure 3, but there is no simple way to correct the individual levels shown in Figure 4. Also, the unoccupied orbitals in tight binding have a different interpretation than those in DFT. Despite these differences, we note that the qualitative shapes of the DFT energy levels in Figure 4 agree better with the orthogonal TB energy levels than the NTB energy levels, as shown in Figures 1b and 2b, although the DFT energy levels have a greater width (i.e., a larger second moment) than those for the TB method.

A final issue that we will look at is how well TB can predict the geometries of small Al clusters. The geometries of small Al_4 and Al_5 are planar,[46−48] and Al_6 is the smallest cluster to have a nonplanar ground state.[46] The ability to correctly predict the correct ground-state geometries of Al_4 and Al_5 with an analytical interatomic potential has proven to be very challenging. The embedded-atom-type models of Ercolessi and Adams[49,50] and Voter and Chen[51,52] predict that Al_4 and Al_5 are three-dimensional. We note that both of these interatomic potentials included the dimer in their fitting strategy. Pettersson et al.[53] have developed analytic interatomic potentials that correctly predict Al_4 and Al_5 to be planar, but the interatomic potential is unphysical for larger clusters. For example, the Pettersson et al.[53] interatomic

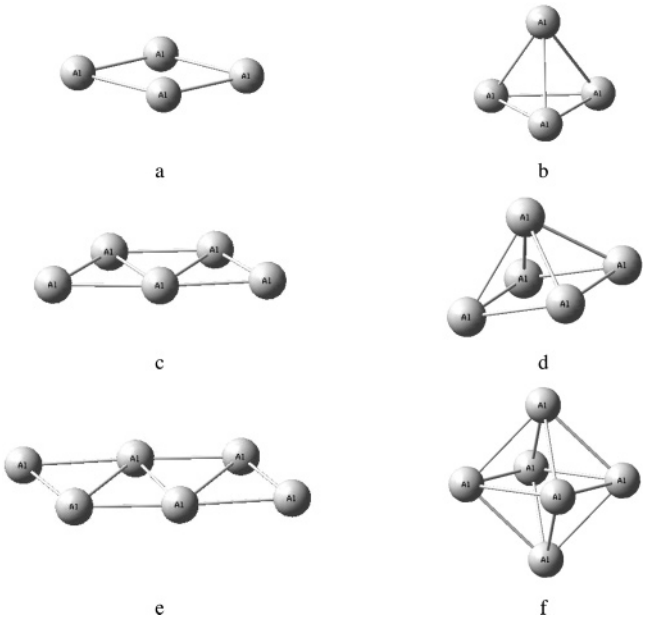

Figure 5. DFT geometries for planar and nonplanar Al_N ($N = 4-6$). The DFT method used for this figure is PBEh/MG3.

Table 4. ΔE (eV) for the Planar to Nonplanar Isomerizations with DFT, TB, and the NP-A and NP-B Interatomic Potentials

method	fitting data	Al_4	Al_5	Al_6
PBEh/MG3		0.24	0.29	−1.06
TB	2	0.18	−0.30	−0.87
	2−177	0.05	−0.26	−0.76
NP-A		−0.59	−1.18	−2.04
NP-B		−0.55	−0.89	−1.89

potential also predicts Al_{13} to be planar and has a 0.7 eV/atom error for the bulk cohesive energy.[53]

We have optimized planar and nonplanar structures for Al_4, Al_5, and Al_6 with the PBEh[44] density functional and the MG3 basis set.[54] The PBEh/MG3 structures are shown in Figure 5. In Table 4 we list the PBEh/MG3, TB, NP-A, and NP-B values for ΔE, and we note that a negative ΔE means that the nonplanar structure is energetically more favorable than the planar structure. The geometries for the TB, NP-A, and NP-B calculations were consistently optimized, and the PBEh/MG3 geometries were the starting points for the TB, NP-A, and NP-B geometry optimizations.

The NP-A and NP-B interatomic potentials both predict a three-dimensional structure for all three cluster sizes (Al_N with $N = 4-6$). The TB method that was fit to the full Al database, with $N = 2-177$, is qualitatively correct for Al_4, and the TB methods are much closer to the PBEh/MG3 values than to the results obtained with the interatomic potentials. These results are encouraging because the simple TB calculations are about three times more accurate than the best analytic functions.

VI. Conclusions

It is well-known that, in simplified methods, overlap-sensitive errors of a similar kind but opposite sign may cancel, and it is desirable to design approximate methods with this in

mind.[59] We have presented several parametrizations for various tight-binding models, and we have investigated the effect of including the overlap in the secular equation and of including many-body terms. We found that one of the simplest models (pairwise orthogonal TB fit to the dimer) is almost as accurate for the entire data set (consisting of 808 geometries from Al_2 to Al_{177}) as the most accurate of the TB fits (orthogonal TB WH+SR). As a general finding, the orthogonal TB model is more accurate than the nonorthogonal model. Many-body terms do not improve the fits in the orthogonal formulations, although they do result in some improvement in the NTB fits when applied to the off-diagonal Hamiltonian matrix elements.

Although the present tests of model types are extensive and systematic, and the results are clear-cut, the tests are restricted to a single element (the only element for which a well-validated data set of nanoparticle energies is available), and we cannot claim that it will always be more accurate to neglect overlap in semiempirical molecular orbital theory or even that it will always be more consistent to neglect it in the special case of tight binding. In fact, although there has been considerable success with orthogonal models, some workers have found, contrary to the results obtained here, that including overlap can reduce the number of parameters and make the parametrizations more transferable.[55,56] But the present results serve as a strong warning that one should not assume that removing approximations (like neglect of overlap) automatically and consistently improves approximate theories. Because including overlap in tight-binding calculations often considerably complicates them and raises the cost,[55,57,58] we recommend that researchers check carefully how much, if any, improvement is afforded by including overlap when they select a model for large-scale computations on nanoparticles, materials, or heterogeneous catalysis.

Acknowledgment. This work is supported in part by the Defense−University Research Initiative in Nanotechnology (DURINT) of the U.S. Army Research Laboratory and the U.S. Army Research Office under agreement number DAAD190110503 and also by the Office of Naval Research under award number N00014-05-1-0538. Computational resources were provided by the Minnesota Supercomputing Institute and by a Grand Challenge Grant at Pacific Northwest National Laboratories.

Supporting Information Available: Tables of the optimized parameters for several of the TB and NTB models. This material is available free of charge via the Internet at http://pubs.acs.org.

References

(1) Lennard-Jones, J. E. *Trans. Faraday Soc.* **1932**, *28*, 334.

(2) Daw, M. S.; Baskes, M. I. *Phys. Rev. B: Condens. Matter Mater. Phys.* **1984**, *29*, 6443.

(3) Jasper, A. W.; Staszewski, P.; Staszewska, G.; Schultz, N. E.; Truhlar, D. G. *J. Phys. Chem. B* **2004**, *108*, 8996.

(4) Jasper, A. W.; Schultz, N. E.; Truhlar, D. G. *J. Phys. Chem. B* **2005**, *109*, 3915.

(5) Streitz, F. H.; Mintmire, J. W. *Phys. Rev. B: Condens. Matter Mater. Phys.* **1994**, *50*, 11996.

(6) Schröder, K.-P.; Sauer, J. *J. Phys. Chem.* **1996**, *100*, 11043.

(7) Hoffmann, R. *J. Chem. Phys.* **1963**, *39*, 1397; **1964**, *40*, 2047, 2474, 2480, 2745.

(8) Slater, J. C.; Koster, G. F. *Phys. Rev.* **1954**, *94*, 1498.

(9) Dewar, M. J. S.; Zoebisch, E. G.; Healy, E. F.; Stewart, J. P. *J. Am. Chem. Soc.* **1985**, *107*, 3902.

(10) Dewar, M. J. S.; Holder, A. J. *Organometallics* **1990**, *9*, 508.

(11) Bredow, T.; Jug, K. *Theor. Chem. Acc.* **2005**, *113*, 1.

(12) Schultz, N. E.; Staszewska, G.; Staszewski, P.; Truhlar, D. G. *J. Phys. Chem. B* **2004**, *108*, 4850.

(13) Wolfsberg, M.; Helmholtz, L. *J. Chem. Phys.* **1952**, *20*, 837.

(14) Staszewska, G.; Staszewski, P.; Schultz, N. E.; Truhlar, D. G. *Phys. Rev. B: Condens. Matter Mater. Phys.* **2004**, *71*, 45423.

(15) Sattelmeyer, K. W.; Jørgensen, W. L. Preprint.

(16) Elstner, M.; Porezag, D.; Jungnickel, G.; Frauenheim, T.; Suhai, S.; Seifert, G. *Phys. Rev. B: Condens. Matter Mater. Phys.* **1998**, *58*, 7260.

(17) Elstner, M.; Porezag, D.; Jungnickel, G.; Frauenheim, T.; Suhai, S.; Seifert, G. *Mater. Res. Soc. Symp. Proc.* **1998**, *491*, 131.

(18) Sattelmeyer, K. W.; Tubert-Brohman, I.; Jorgensen, W. L. *J. Chem. Theory Comput.* **2006**, *2*, 413.

(19) Menon, M.; Richter, E.; Subbaswamy, K. R. *J. Chem. Phys.* **1996**, *104*, 5876.

(20) Jayanthi, C. S.; Wu, S. Y.; Cocks, J.; Luo, N. S.; Xie, Z. L.; Menon, M.; Yang, G. *Phys. Rev. B: Condens. Matter Mater. Phys.* **1998**, *58*, 3799.

(21) Bernstein, N. *Europhys. Lett.* **2001**, *55*, 52.

(22) Sternberg, M.; Galli, G.; Frauenheim, T. *Comput. Phys. Commun.* **1999**, *118*, 200.

(23) Repasky, M. P.; Chandresekhar, J.; Jørgensen, W. L. *J. Comput. Chem.* **2002**, *23*, 1601.

(24) Wang, Y.; Mak, C. H. *Chem. Phys. Lett.* **1995**, *235*, 37.

(25) Foulkes, W. M. C.; Haydock, R. *Phys. Rev. B: Condens. Matter Mater. Phys.* **1989**, *39*, 12520.

(26) Cusachs, L. C.; Cusachs, B. B. *J. Phys. Chem.* **1967**, *71*, 1060.

(27) Lathiotakis, N. N.; Andriotis, A. N.; Menon, M.; Connolly, J. *J. Chem. Phys.* **1996**, *104*, 992.

(28) Lide, D. R. *Handbook of Chemistry and Physics*, 78th ed.; CCR Press: Boca Raton, FL, 1997. Moore, C. E. *Atomic Energy Levels as Derived from the Analyses of Optical Spectra*; Circular of the National Bureau of Standards 467, U.S. Department of Commerce: Washington, DC, 1949; Vol. 1.

(29) Dorantes-Davila, J.; Pastor, G. M. *Phys. Rev. B: Condens. Matter Mater. Phys.* **1995**, *52*, 11837.

(30) Tang, M. S.; Wang, C. Z.; Chan, C. T.; Ho, K. M. *Phys. Rev. B: Condens. Matter Mater. Phys.* **1996**, *53*, 979.

(31) Haas, H.; Wang, C. Z.; Fähnle, M.; Elsässer, C.; Ho, K. M. *Phys. Rev. B: Condens. Matter Mater. Phys.* **1998**, *57*, 1461.

(32) Wang, C. Z.; Pan, B. C.; Tang, M. S.; Haas, H.; Sigalas, M.; Lee, G. D.; Ho, K. M. *Mater. Res. Soc. Symp. Proc.* **1998**, *491*, 211.

(33) Nguyen, D.; Pettifor, D. G.; Vitek, V. *Phys. Rev. Lett.* **2000**, *85*, 4136.

(34) Nguyen-Mahn, D.; Pettifor, D. G.; Vitek, V. *Phys. Rev. Lett.* **2000**, *85*, 4136.

(35) Microgenetic algorithm calculations were carried out using the program Fortran ga, version 1.6.4, as described in: Carroll, D. L. *AIAA J.* **1996**, *34*, 338.

(36) Gollisch, H. *Surf. Sci.* **1986**, *166*, 87.

(37) Papaconstantoupoulos, D. A.; Mehl, M. J. *J. Phys.: Condens. Matter* **2003**, *15*, R413.

(38) Pople, J. A.; Santry, D. P.; Segal, G. A. *J. Chem. Phys.* **1965**, *43*, 5129.

(39) Del Re, G.; Ladik, J.; Carpentieri, M. *Acta Phys. Acad. Sci. Hung.* **1968**, *24*, 391.

(40) Del Re, G.; Molář, M.; Cyrot-Lackmann, F. *J. Phys. (Paris)* **1985**, *46*, 927.

(41) Skinner, A. J.; Pettifor, D. G. *J. Phys.: Condens. Matter* **1991**, *3*, 2029.

(42) Pettifor, D. G.; Aoki, M. In *Equilibrium Structure and Properties of Surfaces and Interfaces*; Gonis, A., Stocks, G. M., Eds.; Plenum: New York, 1992; pp 123−137.

(43) Canel, L. M.; Carlsson, A. E.; Fedders, P. A. *Phys. Rev. B: Condens. Matter Mater. Phys.* **1993**, *48*, 10739. McKinnon, B. A.; Choy, T. C. *Phys. Rev. B: Condens. Matter Mater. Phys.* **1995**, *52*, 14531. Yang, S. H.; Mehl, M. J.; Papaconstantopoulos, D. A. *Phys. Rev. B: Condens. Matter Mater. Phys.* **1998**, *57*, R2013. Mehl, M. J.; Papaconstantopoulos, D. A. *Phys. Rev. B: Condens. Matter Mater. Phys.* **2000**, *61*, 4894. Frøseth, A. G.; Holmestad, R.; Derlet, P M.; Marthinsen, K. *Phys. Rev. B: Condens. Matter Mater. Phys.* **2003**, *68*, 12105. Rittenhouse, S. T.; Johnson, B. L. *Phys. Rev. B: Condens. Matter Mater. Phys.* **2005**, *71*, 35118.

(44) Perdew, J. P.; Burke, K.; Ernzerhof, M. *Phys. Rev. Lett.* **1996**, *77*, 3865; **1997**, *78*, 1396 (E).

(45) Schultz, N. E.; Truhlar, D. G. *J. Chem. Theory Comput.* **2005**, *1*, 41.

(46) Bauschlicher, C. W., Jr.; Pettersson, L. G. M. *J. Chem. Phys.* **1987**, *87*, 2198.

(47) Geske, G.; Boldyrev, A. I.; Li, X.; Wang, L.-S. *J. Chem. Phys.* **2000**, *113*, 5130.

(48) Zhan, C.-G.; Zheng, F.; Dixon, D. A. *J. Am. Chem. Soc.* **2004**, *124*, 14795.

(49) Ercolessi, F.; Adams, J. *Europhys. Lett.* **1993**, *26*, 583.

(50) Doye, J. P. K. *J. Phys. Chem.* **2003**, *119*, 1136.

(51) Voter, A. F.; Chen, S. P. *Mater. Res. Soc. Symp. Proc.* **1987**, *82*, 175.

(52) Sebetci, A.; Güvenç, Z. B. *Modell. Simul. Mater. Sci. Eng.* **2005**, *13*, 683.

(53) Pettersson, L. G. M.; Bauschlicher, C. W., Jr.; Halicioglu, T. *J. Chem. Phys.* **1987**, *87*, 2205.

(54) Fast, P. L.; Sánchez, M. L.; Truhlar, D. G. *Chem. Phys. Lett.* **1999**, *306*, 407.

(55) Dorantes-Dávila; Pastor, G. M. *Phys. Rev. B: Condens. Matter Mater. Phys.* **1994**, *51*, 16627.

(56) Menon, M.; Subbaswamy, K. R. *Phys. Rev. B: Condens. Matter Mater. Phys.* **1997**, *55*, 9231.

(57) Jayanthi, C. S.; Wu, S. Y.; Cocks, J.; Luo, N. S.; Xie, X. L.; Menon, M.; Yang, G. *56. Phys. Rev. B: Condens. Matter Mater. Phys.* **1998**, *57*, 3799.

(58) Steinberg, M.; Galli, G.; Frauenheim, T. *Comput. Phys. Commun.* **1999**, *118*, 200.

(59) Pople, J. A.; Segal, G. A. *J. Chem. Phys.* **1966**, *44*, 3289.

CT600261S